

## High Temperature Testing of Materials and Corrosion Resistant Coatings for Geothermal Drilling Applications

Erlend Oddvin Straume<sup>a</sup>, Gifty Oppong Boakye<sup>a</sup>, Beatriz Alonso Rodriguez<sup>c</sup>, Sigrún Nanna Karlsdóttir<sup>a,b</sup>

<sup>a</sup>Department of Industrial Engineering, Mechanical Engineering and Computer Science, University of Iceland, Reykjavik, Iceland

<sup>b</sup>Gerosion Ltd., Árleynir 2-8, IS-112 Reykjavik, Iceland

<sup>c</sup>Graphenea, SA, Mikeletegi 83 A75022608, Donostia-San Sebastian, 20009, Spain

[erlend@hi.is](mailto:erlend@hi.is), [gob13@hi.is](mailto:gob13@hi.is), [b.alonso@graphenea.com](mailto:b.alonso@graphenea.com), [snk@hi.is](mailto:snk@hi.is)

**Keywords:** CO<sub>2</sub>/H<sub>2</sub>S Corrosion; High Temperature Corrosion; Geothermal Environment; Geo-Drill; Graphene-Oxide-Polymer coatings.

### ABSTRACT

Through the development and improvement of drilling methods and equipment, the Geo-Drill project aims to save time and reduce costs during drilling of geothermal wells. New materials and corrosion resistant coatings have been fabricated and tested in a 3 L high pressure and high temperature (HTHP) autoclave in the newly installed corrosion laboratory at the University of Iceland at pressure, temperature, and chemical conditions equivalent to those of a geothermal well. The aggressive geothermal environment requires the development of cost-effective corrosion resistant coatings and materials for drilling equipment and instrumentation to increase service life. The materials fabricated for the novel drilling equipment and sensors developed in the Geo-Drill project, include graphene oxide-based coatings, high entropy alloy and cermet coatings. Within the project, high temperature corrosion experiments were performed, here we report the results from an experiment designed to simulate harsh conditions that can be encountered during geothermal well drilling if loss of circulation of the drilling fluid occurs with the subsequent ingress of H<sub>2</sub>S and CO<sub>2</sub> gases. The experiment was conducted at 250 °C with a 50 bar pressure in water (vapor and liquid phases) with CO<sub>2</sub>, H<sub>2</sub>S gasses introduced to simulate the geothermal environment. The duration of the tests was 7 days. Here we describe the design of the HTHP corrosion testing facility and report on the results from the corrosion testing of a novel graphene oxide (GO)-containing polymer coatings. Microstructural and chemical composition analyses were performed with scanning electron microscope with an attached energy-dispersive X-ray spectroscopy equipment before and after testing to investigate the corrosion resistance of the GO added polymer coatings. Weight changes were also measured to evaluate the stability at high temperatures and corrosion resistance.

### 1. INTRODUCTION

The corrosive nature of the geothermal environment, particularly the effects of high temperature and chemical composition of the geothermal fluid on steel and iron alloys, leads to corrosion damage of drilling equipment, well casing and other parts of the geothermal plant facilities, which decreases their service life. Hydrogen sulfide (H<sub>2</sub>S) and carbon dioxide (CO<sub>2</sub>) present in geothermal systems are the main reasons for the corrosion effects (Karlsdóttir, 2012). Aggressive chloride [Cl<sup>-</sup>] and sulfate [SO<sub>4</sub><sup>2-</sup>] ions are also to some degree present in geothermal fluids (Stefánsson, 2017) and can increase corrosion rate and facilitate localized corrosion such as pitting corrosion and crevice corrosion. In general, the corrosion rate for carbon steel increases in environments with pH levels lower than 7 (Karlsdóttir, 2012), whereas passive film forms on carbon steel in pH ranging from 9.5 to 14, which leads to a decrease in the corrosion rate (Kovalov et al., 2019).

Geothermal drilling environment is extremely harsh in terms of temperature, pressure, rock breaking, etc. Components of the geothermal systems are subjected to corrosion, material fatigue, wear, and erosion. The project Geo-Drill aims to develop novel and cost-effective drilling technology for geothermal systems. Part of this is the development of novel coatings to improve wear resistance corrosion resistance and high temperature stability. In the Geo-Drill project, Graphene Oxide (GO)-PTFE based coatings have been developed by Graphenea for DTH hammer and sensor system (European Commission, 2019) to improve wear and erosion resistance of these components as a key parameter to improve their service life. Studies show that the addition of GO combined with polyurethanes dramatically improves the anti-corrosive performance of polyvinylidene difluoride coatings (Xiao et al., 2017). PTFE (Polytetrafluoroethylene) is a synthetic polymer widely used in many applications due to its chemical inertness, durability, high capacity of insulating, dielectric properties, among others. GO is a bi-dimensional material produced by the strong oxidation of graphite. This oxidation introduces oxygen moieties in the structure making the GO compatible with a wide range of matrices while at the same time increasing the interlayer distance between flakes to easily obtain monolayer sheets. The high aspect ratio of the GO leads to an improvement of properties by adding small amounts of the material. Nemati et al. (Nemati et al., 2016), for example, observed that by the addition of GO to PTFE at 15 vol%, the wear rate decreased from  $5.6 \times 10^{-8}$  to  $1.9 \times 10^{-9}$  mm<sup>3</sup> N<sup>-1</sup> m<sup>-1</sup> and at the same time the coefficient of friction was reduced from 0.16 to 0.045 in the micro-scale while this improvement was not so dramatic in the macro-scale.

This paper presents results from high pressure – high temperature (HPHT) corrosion experiments with carbon steel coated graphene-oxide-polymer coatings with various content of graphene oxide. The experiments were performed in the newly installed HPHT autoclave corrosion laboratory at the University of Iceland. The coupon samples were tested at conditions to simulate a particular drilling scenario: unplanned shut-down (drill stuck in well) for one week with leakage of geothermal fluid containing dissolved H<sub>2</sub>S and CO<sub>2</sub> into the well at 250 °C and 50 bar.

## 2. EXPERIMENTAL

### 2.1 Experimental setup

The University of Iceland has recently installed a laboratory capable of conducting high-temperature and high-pressure experiments with geothermal fluids (Figure 1). The laboratory was designed and constructed by Cormet Oy, Finland. Gas detection and alarm systems were installed in the laboratory to ensure safe operation for experiments with  $\text{H}_2\text{S}$  and  $\text{CO}_2$  gas. The central equipment in this laboratory is a 3 L autoclave made of c 276 Hastelloy and rated for temperatures up to 500 °C and pressures up to 300 bar (Figure 2). The autoclave lid is fitted with a custom-made stirrer impeller connected to a Top Industrie magnetic stirrer. The custom-made sample holder is also installed in the lid, and during the experiment, the test samples are installed between the vertical sample holder supports. The lid is controlled by a lifting mechanism, and during experiments, it is lowered and connected with 9 bolts to the autoclave vessel. Temperature is measured with a Pt100 temperature sensor and pressure is measured with a Keller pressure transmitter in the vessel. The temperature is controlled by heating elements around the autoclave vessel and the lid of the autoclave is insulated during experiments (Figure 3). Water can be drained from the bottom of the autoclave. The autoclave can be pressurized from the bottom with  $\text{N}_2$ ,  $\text{H}_2\text{S}$  and  $\text{CO}_2$  through the gas inlet lines. The gas components are fed through the gas filling panel (Figure 3, right part of the photo) with the filling rate controlled by Brooks mass flow controllers. The autoclave can be depressurized through a gas draining line in the top. The gas drained from the autoclave flows into three 20 L plastic containers (shown in the left part of the photo in Figure 3), filled with a water-based solution with  $\text{pH} = 13.5$  containing dissolved zinc acetate and  $\text{NaOH}$ .  $\text{H}_2\text{S}$  gas from the autoclave react with the zinc acetate and form solid  $\text{ZnS}$  that precipitates out of the solution and sinks to the bottom of the plastic containers.



**Figure 1: The corrosion laboratory constructed in a modified 40-foot high-cube container by Cormet Oy, Finland, shipped to Iceland, and installed at the campus of the University of Iceland.**



**Figure 2:** The autoclave with the lid opened before installation of test samples in the sample holder.



**Figure 3:** The autoclave experimental setup, including gas filling station (right) and H<sub>2</sub>S capture system (left).

## 2.2 Materials

Different coatings were applied to standard carbon steel (CS) substrates of 50 x 25 x 3 mm coupons (Figures 4 and 5). The PTFE based coating also includes PPS which was mixed with different weight fractions of graphene oxide (GO) to fabricate the composite-coatings received from Graphenea SA. Results from testing of the following three coatings are reported in this study: CS coated with PTFE-PPS coating with no GO added (herein referred to as 0wt%GO coating), CS coated with PTFE-PPS and 0.5wt.% GO (0.5wt%GO coating) and CS coated with PTFE-PPS and 2.5wt.% GO (2.5wt%GO coating).

Graphene oxide was produced using a modified Hummers method (GRAPHENEA's methodology: patent EP15382123 2015): graphite powder was dispersed and cooled down in H<sub>2</sub>SO<sub>4</sub>. KMnO<sub>4</sub> was then added to the mixture. After stirring for 1h, the mixture was heated up to 30°C and kept at this temperature. The mixture was cooled down and distilled water was slowly added to the slurry. Finally, H<sub>2</sub>O<sub>2</sub> was added and this dispersion was purified by cleaning with distilled water obtaining the GO slurry (water dispersion). Commercial PTFE-PPS coating was used as a reference for this study. To prepare the PTFE-PPS /GO blends, the necessary amount of GO slurry was added to the PTFE-PPS and dispersed in a Dispermat system at velocities from 600 to 1000 rpm during 15-30 min. The CS substrates were spray-coated with the PTFE-PPS /GO mixtures and cured at 400°C for 10min.

## 2.3 Experimental procedure

Before an experiment, the insides of the autoclave vessel were cleaned with acetone and ethanol. The coupon samples (Figures 4 and 5) were weighed and installed in the vertical sample holder supports as shown in Figure 6. A 1.5 L of deionized water with 0.60 g of NaOH and 0.44 g of NaCl dissolved in the water was filled into the vessel. The NaOH and NaCl were added to maintain a stable neutral pH after filling H<sub>2</sub>S, CO<sub>2</sub> and N<sub>2</sub> and heating to 250 °C. Samples were tested in both liquid phase and vapor phase in this experiment. The upper row of samples shown in Figure 6 were located in the vapor phase and the lower row samples were submerged in the liquid phase during the test since the 3 L autoclave was only half-filled. After installation of the samples and filling of water, the lid of the autoclave was lowered to seal the autoclave vessel and the 9 bolts were tightened with 250 Nm torque. The autoclave was pressurized to 50 bar, with nitrogen at 25 °C for one day to check for leakage for safety purposes. The data logging system recorded the pressure and temperatures measured during the leakage test. The stirrer rotation speed was set to 60 RPM.



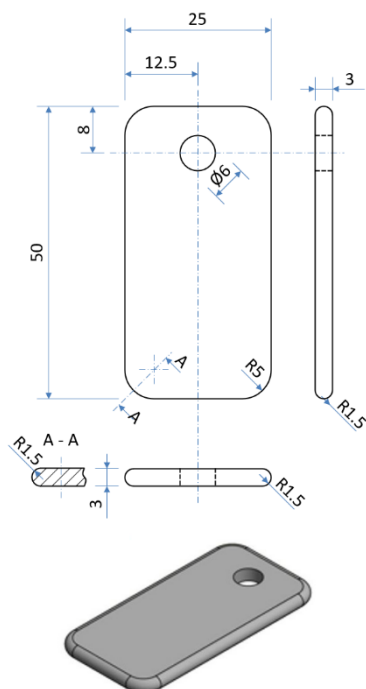


**Figure 4: Drawing of Coupon samples for the corrosion tests.**



**Figure 5: Coupon sample from Graphenea prepared for the corrosion tests.**

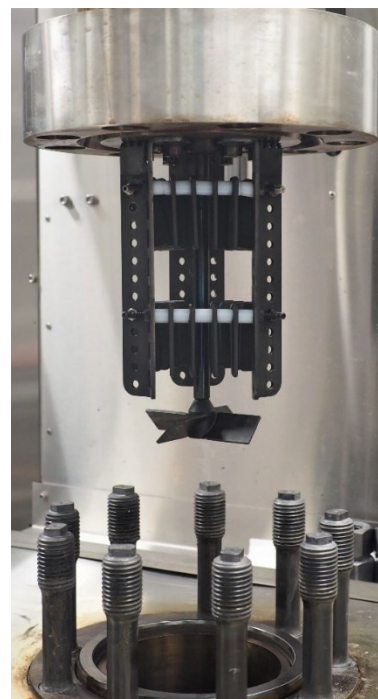


**Figure 6: Coupon samples installed in the autoclave.**

After successful completion of the leakage test prior to the 250 °C test, the pressure was lowered to 0 bar before filling the gasses. The autoclave vessel was filled with 1.07 g of H<sub>2</sub>S, 11.05 g of CO<sub>2</sub> and 7.04 g of N<sub>2</sub>. The H<sub>2</sub>S, CO<sub>2</sub> and N<sub>2</sub> gases used in the experiment were all of purity 99.5% and delivered by Linde Gas. The filling was controlled and measured by Brooks mass flow controllers and values logged by the data logging program. Following the filling procedure, the H<sub>2</sub>S gas bottle was closed and the H<sub>2</sub>S gas filling lines and capture system were flushed carefully with N<sub>2</sub> gas to ensure that during the experiment, no H<sub>2</sub>S could leak into the working space of the laboratory. The logging of the experiment was started, and the autoclave was heated to 250 °C at a rate of 25 °C/h with lower heating rate as the temperature approached 250 °C. The calculated composition of the solution after filling and heating to 250 °C is reported in Table 1, and the calculated composition of the vapor phase after filling and heating to 250 °C is reported in Table 2.

**Table 1: Principle chemical components dissolved in the water phase at 250 °C and 50 bar calculated by using Peng-Robinson chemical model in Phreeqc (Phreeqc Users, 2020).**

CO <sub>2</sub> [mg/kg]	HCO <sub>3</sub> <sup>-</sup> [mg/kg]	H <sub>2</sub> S [mg/kg]	HS <sup>-</sup> [mg/kg]	N <sub>2</sub> [mg/kg]	Na <sup>+</sup> [mg/kg]	Cl <sup>-</sup> [mg/kg]
1981	393	472	99	292	350	181

**Table 2: Chemical composition of vapor phase calculated by Peng-Robinson calculation using a chemical model in Phreeqc (Phreeqc Users, 2020).**

H <sub>2</sub> O [mol%]	CO <sub>2</sub> [mol%]	H <sub>2</sub> S [mol%]	N <sub>2</sub> [mol%]
79.8	8.5	0.3	11.4

After an experiment, the autoclave was cooled from the experimental temperature to room temperature at a rate of 25 °C/h, then slowly depressurized after cooling. The autoclave was flushed carefully with N<sub>2</sub> gas to ensure that no H<sub>2</sub>S was present in the autoclave at the time it was opened. A solution of 11 g of zinc acetate dissolved in 0.5 L of water was prepared and mixed into the remnant solution in the autoclave vessel after the lid with the tested samples had been removed. This ensured that all remaining sulfur dissolved in the water precipitated as ZnS. After that, the water was drained out of the autoclave. The samples were then removed from the holder and the weighed. The microstructure and chemical composition of the tested GO-polymer coatings were studied using SEM/EDS analysis.

### 3. RESULTS AND DISCUSSION

#### 3.1 Weight change and visual appearance before and after tests

The quantity of corrosion and deposited corrosion products on the samples were measured by weight change. Table 3 presents the average weight gain of each samples tested under the two different test conditions: vapor phase containing H<sub>2</sub>S, CO<sub>2</sub> and N<sub>2</sub> at 250 °C and 50 bar, and liquid phase containing NaOH, NaCl, CO<sub>2</sub> and H<sub>2</sub>S, pH =7 at 250 °C, 50 bar. Three samples of each coating were tested in vapor and water phase. Standard deviation for weight change within each group of samples were 17% or less for all groups except the 2.5% GO samples tested in the water phase at 250 °C, 50 bar, which had a standard deviation of 83%. The results presented

in Table 3 show that the samples with 0.5% GO – PTFE coating had the smallest average weight change and the samples with 2.5% GO – PTFE coating had the largest weight change for all tested conditions. The weight increased for all samples tested in the simulated geothermal environment with H<sub>2</sub>S and CO<sub>2</sub> present. This might be explained by the formation of iron sulfide on the surface of the samples as discussed in the microstructural and chemical composition analysis.

**Table 3: Measured average weight change for three different coatings tested at the 250 °C in liquid vs. steam conditions.**

GO %	Average weight change of each samples type (mg)	
	Vapor phase 250 °C	Liquid (water) phase 250 °C
0	28.3	26.9
0.5	19.3	11.1
2.5	42.3	31.2

Figures 7 and 8 present photos of samples coated with 0%, 0.5% GO – PTFE and 2.5% GO – PTFE based coatings before and after the tests for the two experimental conditions. These photos show considerable difference in the visual appearance of the corrosion behavior of the samples with 0% GO – PTFE and 2.5% GO – PTFE coatings compared to 0.5% GO – PTFE coating.



**Figure 7: Photos of coupon samples with 0%, 0.5% and 2.5% GO – PTFE coatings un-tested (new) and after 250 °C corrosion tests in vapor phase.**



**Figure 8: Photos of coupon samples with 0%, 0.5% and 2.5% GO – PTFE coatings un-tested (new) and after 250 °C corrosion tests in liquid phase.**

### 3.2 Microstructural and chemical composition analysis of coatings

Figure 9 shows the SEM images of the microstructure of the surface of the 0wt%GO-PTFE/PPS coating before and after testing in liquid and vapor phase. As can be seen from the comparison of the un-tested coating, there is a visible change in the microstructure of the coating after testing, and more pronounced effects in the vapor phase where the non-condensable gases (NCG), the H<sub>2</sub>S and CO<sub>2</sub> are present during the testing. Large iron (Fe) and sulfur (S) rich crystals have formed on the surface and the amount of fluorine (F) decreased. This is obvious in Figure 10, showing the distribution of elements with the EDS maps obtained in the chemical



compositional analysis in the SEM with EDS analyzer. The increased amount of Fe and S and decrease in F compared to the non-tested sample indicates that the 0wt%GO-PTFE/PPS coating is not effective in protecting the substrate from corrosion by H<sub>2</sub>S and CO<sub>2</sub> at high temperatures. This is confirmed from the EDS results shown in Figures 10 and 11.

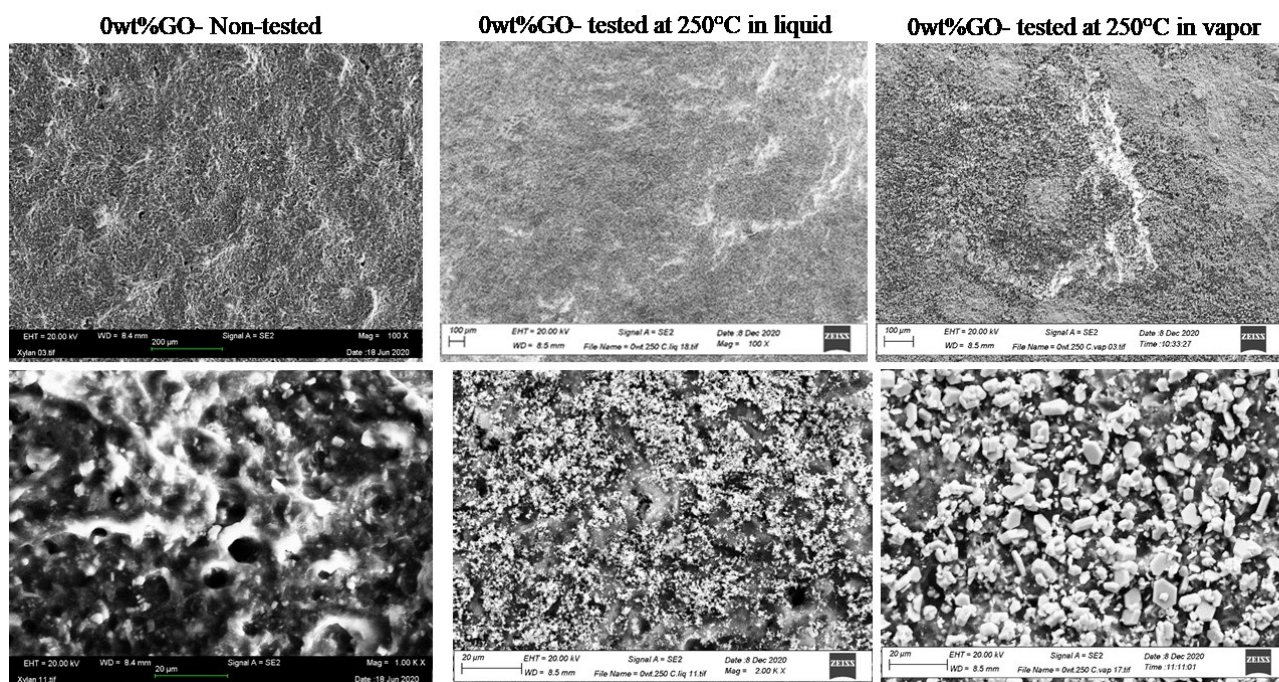


Figure 9: SEM images showing the microstructure of the 0wt%GO-PTFE based coating at low and high magnification.

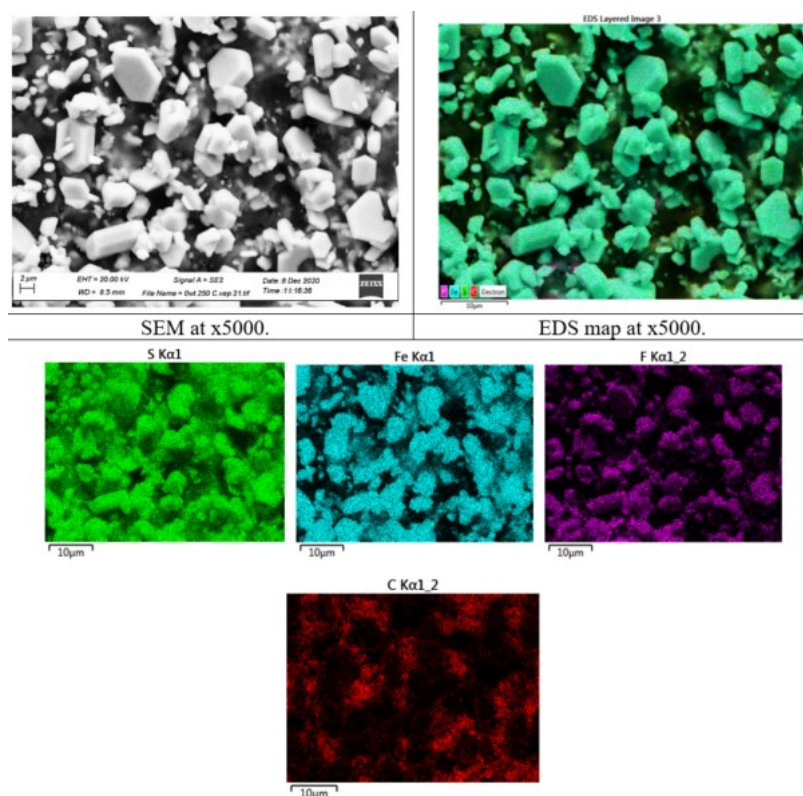
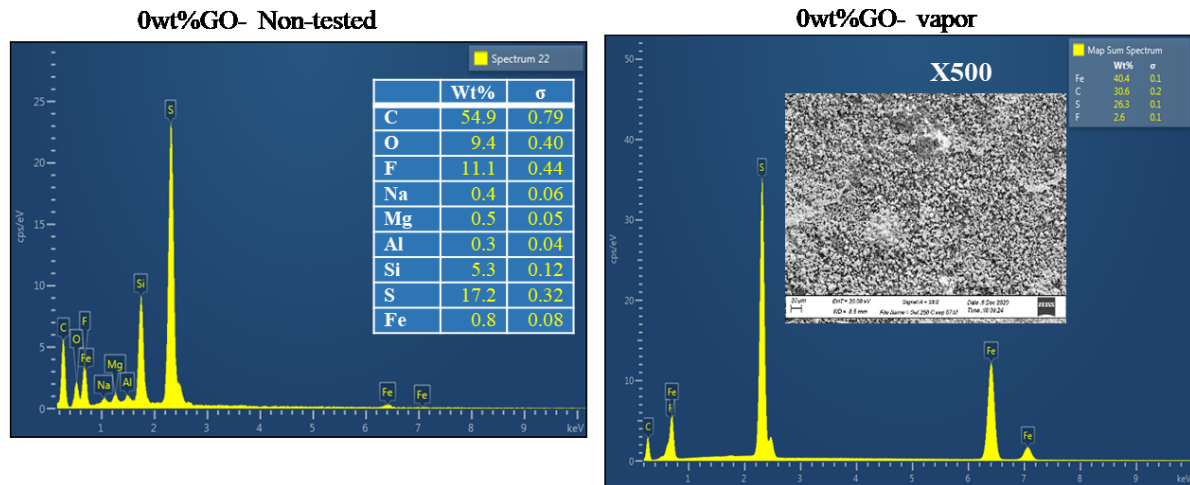
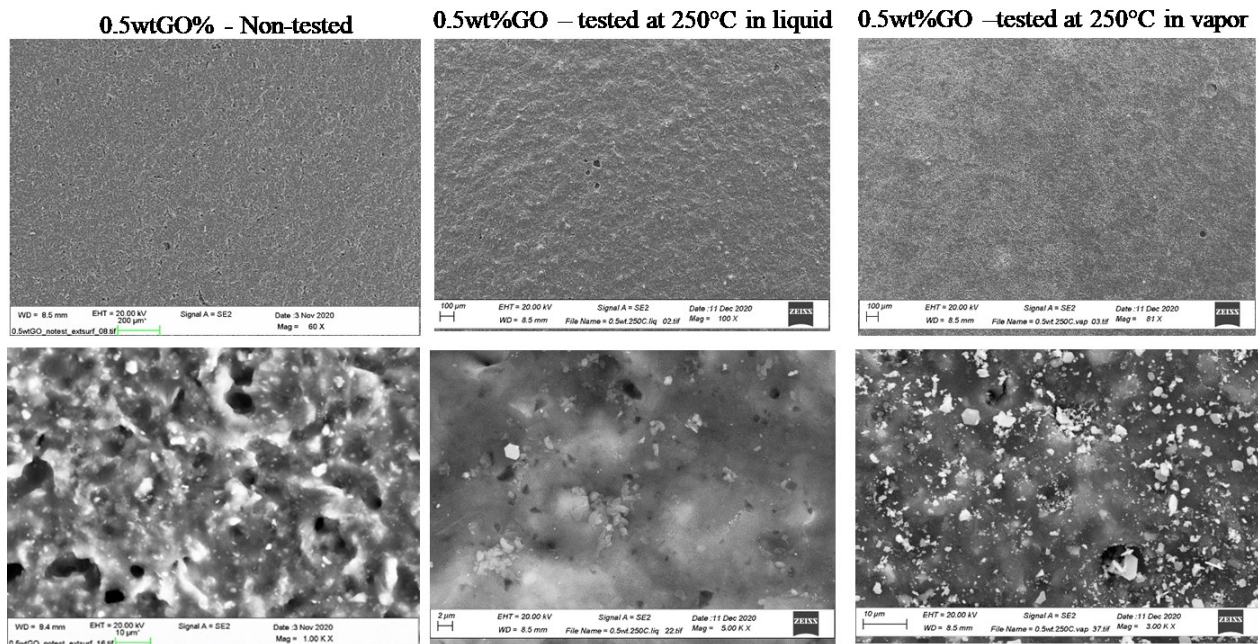


Figure 10: SEM image of the 0wt% GO-PTFE based coating and EDS elemental maps of the area shown in the SEM image.



**Figure 11: EDS spectrum of the area shown in the micrographs for the 0wt% GO-PTFE based coating untested (left) and tested at 250°C vapor conditions (right) in the autoclave.**



**Figure 12: SEM images showing the microstructure of the 0.5wt%GO-PTFE based coating at low and high magnification.**

Figure 12 shows the SEM images of the microstructure of the surface of the 0.5wt% GO-PTFE/PPS coating before and after testing in the liquid and vapor phase. As can be seen from the comparison of the un-tested coating, there is not as much visible change in the microstructure of the coating after testing as for the 0wt%GO. There are more changes in the morphology of the surface after the vapor phase testing of the 0.5wt% GO-PTFE/PPS compared to the liquid phase testing. Few Fe, S rich crystals were detected on the surface, as can be seen in Figure 12 and Figure 13, showing the elemental maps of 0.5wt% GO-PTFE/PPS sample tested in the vapor phase. The amount of F did not decrease as well and there was only a small increase in Fe and S, indicating better performance of the coating in protecting the carbon steel substrate material.



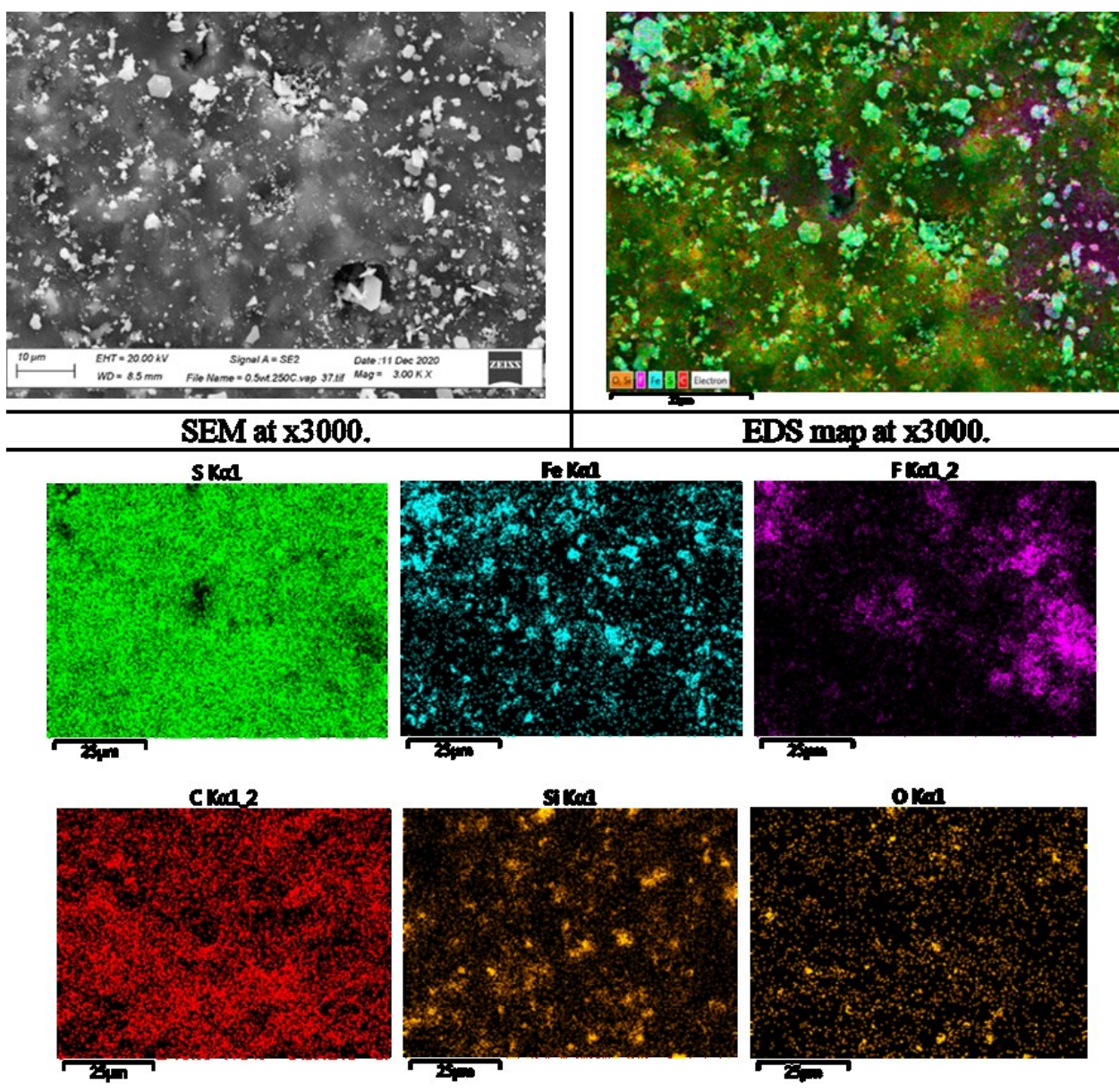
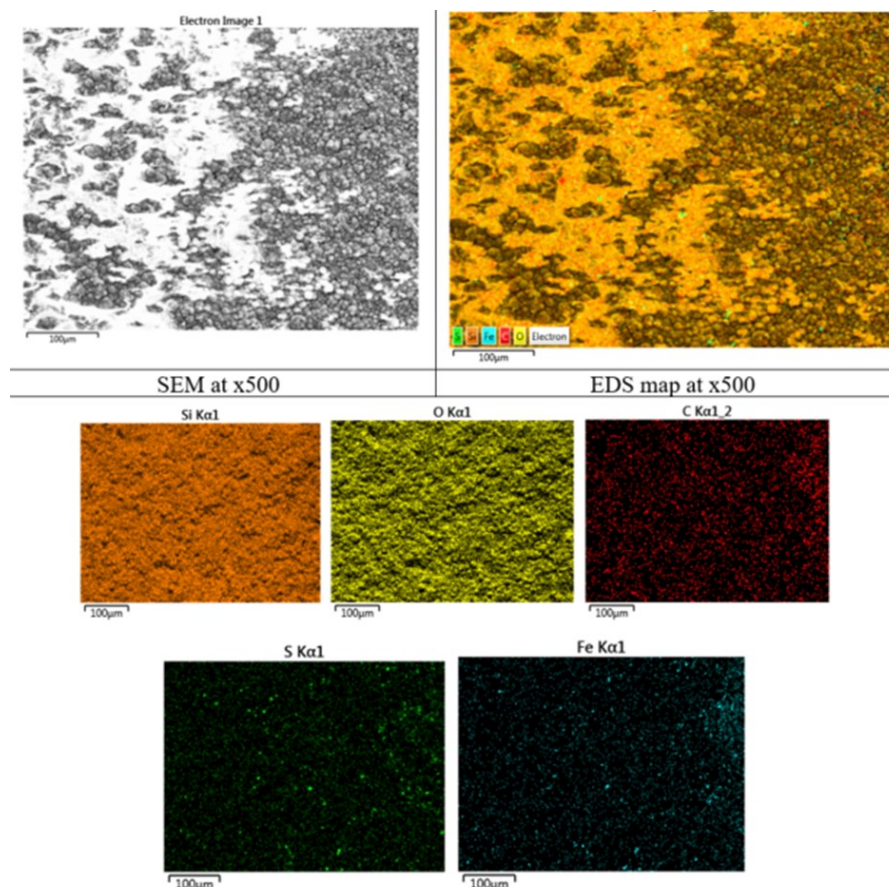


Figure 13: SEM image of the 0.5wt% GO-PTFE based coating and EDS elemental maps of the area shown in the SEM image.

Also, some silica ( $\text{SiO}_2$ ) was detected originating from the tap water used, as drilling fluid is commonly based on cold tap water available at drilling sites, which can contain  $\text{SiO}_2$  or other dissolved minerals. Figure 14 shows EDS maps confirming  $\text{SiO}_2$  deposit on the 0.5wt%GO-PTFE/PPS coating in the liquid phase.





**Figure 14: SEM image of the surface of the 0.5wt% GO-PTFE based coating tested at 250°C in vapor in the autoclave and EDS elemental maps of the area shown in the SEM image.**

The performance of the 2.5wt% GO-PTFE based coating in the corrosion tests was similar to the 0wt% GO-PTFE with high amount of iron sulfur rich products formed on the surface; indicating that higher content of GO nanoparticles does not improve the corrosion resistance. This is in line with previously reported results on the effects GO addition on the microstructure of a PTFE/PPS polymer coating, where increased GO content above 1wt% (2.5wt% and 5wt%) resulted in micro-cracks in the polymer coating and porous and thin coating (Boakye et al., 2021 paper, Zhang et al., 2020). Figure 15 shows the SEM images of the surface of the 2.5wt%GO-PTFE/PPS coating un-tested and after testing in the liquid and vapor phase. As can be seen in the micrograph for the non-tested sample micro-cracks are present which will allow easy diffusion of corrosive species and gases into the coating.

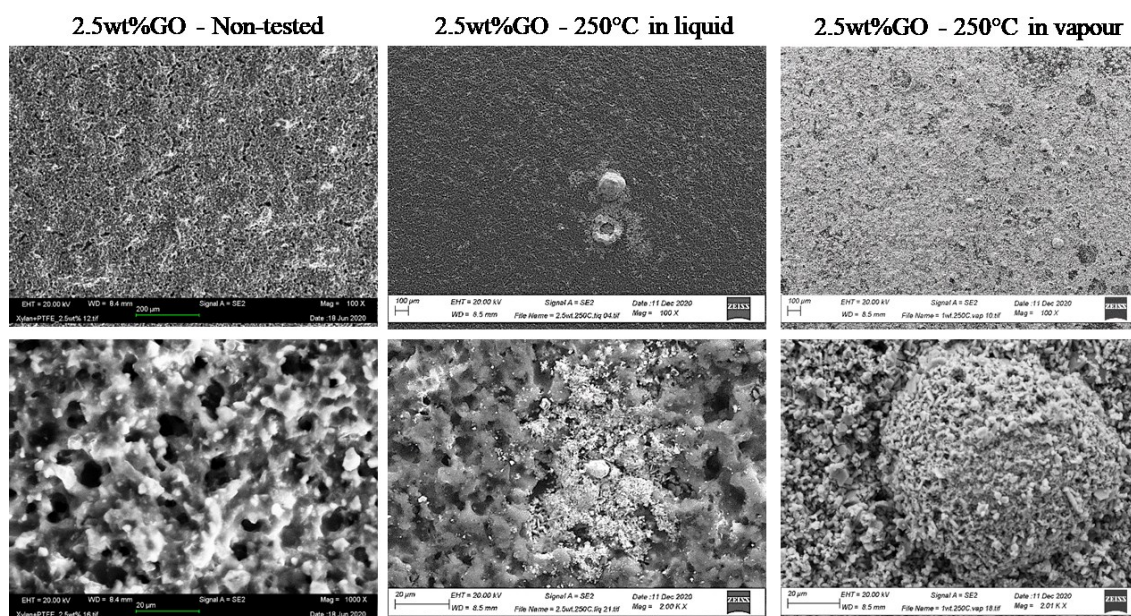


**Figure 15: SEM images showing the microstructure of the surface of the 2.5wt%GO-PTFE based coating at low and high magnification un-tested and after corrosion testing.**



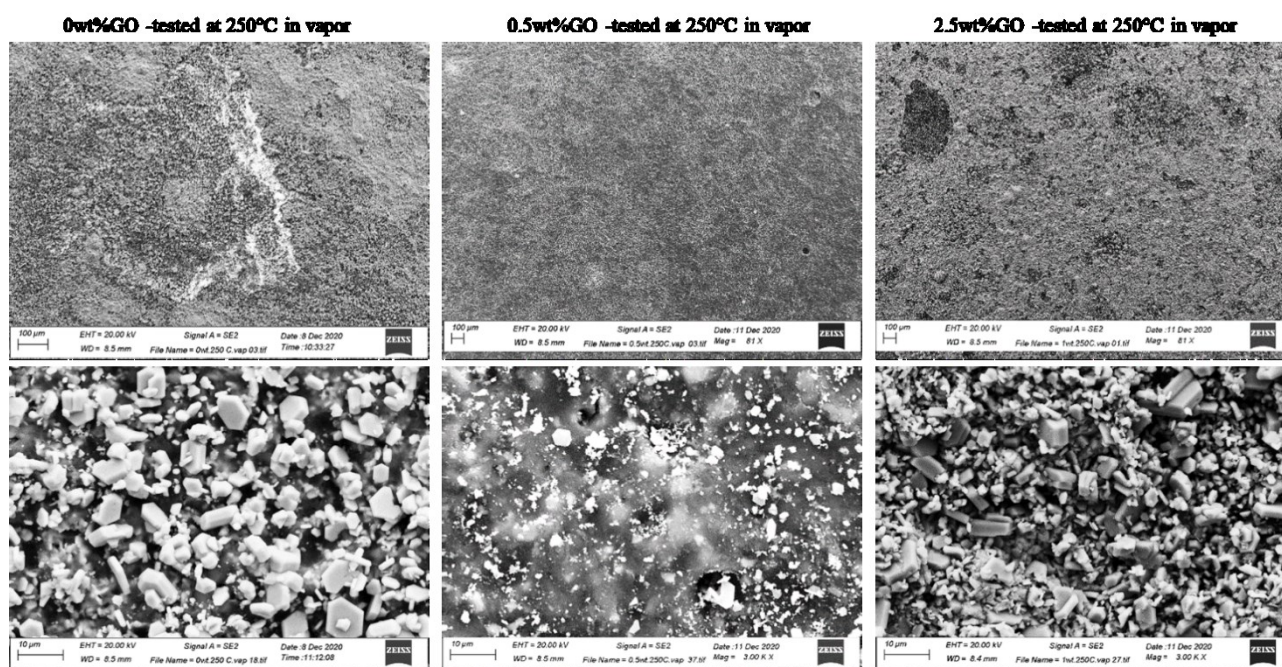


**Figure 16: SEM images showing the microstructure of the surface of the 0wt%, 0.5wt% and 2.5wt% GO-PTFE based coating tested in vapor condition at 250°C.**

Figure 16 shows the SEM images of the surfaces of the 0wt%, 0.5wt% and 2.5wt% GO-PTFE/PPS based coatings tested in vapor condition at 250°C. As can be seen by comparing the images, the 0.5wt% is the least affected, which is in line with the weight analysis reported in Table 3, where the 0.5wt% showed overall the lowest weight gain indicating best performance in protecting the carbon steel substrate.

#### 4. CONCLUSIONS

In this work, we present the newly installed HPHT autoclave laboratory facility at University of Iceland for conducting corrosion tests for novel coatings for geothermal applications. Carbon steel sample coupons coated with a PPS-PTFE blend mixed with different weight fractions of graphene oxide (GO) were exposed to vapor and liquid phase containing  $H_2S$ ,  $CO_2$  and  $N_2$  at 250 °C and 50 bar for 7 days to simulate leakage of geothermal fluid during drilling operations. Recorded weight of the test coupons before and after exposure indicated that coupons with the 0.5wt% GO coating had the lowest weight gain while the 2.5wt%GO-PTFE/PPS coated coupons had the highest weight gain. Increased weight gain indicates more FeS formation from corrosion of carbon steel substrate which is consistent with the results from the microstructural and chemical compositional analysis of the surfaces of the tested corrosion coupons.

The results indicate that a small quantity of GO nano-particles positively affects corrosion resistance of the PTFE-PPS coating. Nevertheless, higher concentration of GO introduces cracks in the microstructure of the coating affecting corrosion resistance negatively by allowing more rapid diffusion of elements/corrosive species.

#### 5. ACKNOWLEDGEMENT

This work is part of the H2020 EU project Geo-Drill: “Development of novel and cost-effective drilling technology for Geothermal Systems” funded by H2020 EU project no. 815319. The authors would also like to acknowledge the resources and collaborative efforts provided by the consortium of the Geo-Drill project.

#### REFERENCES

- Karlsdóttir, S.N.: Corrosion, Scaling and Material Selection in Geothermal Power Production, in: *Compr. Renew. Energy*, (2012).
- Stefánsson, A.: Gas chemistry of Icelandic thermal fluids, *J. Volcanol. Geotherm. Res.* 346 (2017) 81–94.
- Kovalov, D., Ghanbari, E., Mao, F., Kursten, B., Macdonald, D.D.: Investigation of artificial pit growth in carbon steel in highly alkaline solutions containing 0.5 M NaCl under oxic and anoxic conditions, *Electrochimica Acta*. 320 (2019).
- European Commission, Innovation and Networks Executive Agency: Grant Agreement Number 815319 — Geo-Drill, Ref. Ares(2019)1399863 - 01/03/2019.
- Xiao, Y.-K., Ji, W.F., Chang, K.-S., Hsu, K.-T., Yeh, J.-M., Liu, W.-R.: Sandwich-structured rGO/PVDF/PU multilayer coatings for anti-corrosion application, *RSC Advances*, 7, (2017), 33829–33836.
- Nemati, N., Emamy, M., Yau, S., Kimbc, J.-K., Kim, D.-E.: High temperature friction and wear properties of graphene oxide/polytetrafluoroethylene composite coatings deposited on stainless steel, *RSC Advances*, 6, (2016), 5977–5987.
- Elorza, A.Z., Rodríguez, B.A.: Method for obtaining graphene oxide, *European Patent Office*, (2015), EP15382123.6A



Phreeqc Users, Phreeqc, open-source program, <https://phreeqcusers.org>, accessed 2020.

Zhang, F., Begg, H., Kale, N., Irukuvarghula, S., Franklin, K., Mallin, K., Wittig, V., Hahn, S., Rodriguez, B.A., Chowdhury, F., Hoque, M.A., Karlsdóttir, S.N., Boakye, G.O., Kjellgren, P., Obene, P., Alexandersson, K.F., Wallevik, S.Ó.: Geo-Drill: Development of novel and cost-effective drilling technology for geothermal systems, Proceedings World Geothermal Congress 2020 - submitted

Boakye, G.O., Kovalov, D., Straume, E.O., Karlsdottir, S.N., Rodriguez, B.A.: Microstructural Characterization, Corrosion and Wear Properties of Graphene Oxide Modified Polymer Coatings for Geothermal Drilling Applications, *National Association of Corrosion Engineers*, Proceedings NACE 2021 conference - submitted